

NuSTAR observation of the Arches cluster: X-ray spectrum extraction from a 2D image

Roman Krivonos^{*†}

Space Research Institute (IKI), Moscow, Russia

E-mail: krivonos@iki.rssi.ru

The *NuSTAR* mission performed a long (200 ks) observation of the Arches stellar cluster in 2015. The emission from the cluster represents a mixture of bright thermal ($kT \sim 2$ keV) X-rays and the extended non-thermal radiation of the molecular cloud around the cluster. In this work we describe the method used to decouple spatially confused emission of the stellar cluster and the molecular cloud in the *NuSTAR* data.

*11th INTEGRAL Conference Gamma-Ray Astrophysics in Multi-Wavelength Perspective
10-14 October 2016
Amsterdam, The Netherlands*

*Speaker.

†A footnote may follow.

1. Introduction

The Arches cluster is a young, densely packed massive star cluster in our Galaxy that shows a high level of star formation activity. It is located in the inner Galactic Center (GC) region at the projected distance of 11' from the position of the dynamic center of the Galaxy – Sagittarius A*.

The Arches cluster is a known source of thermal and non-thermal X-ray emission. The thermal emission is thought to originate from multiple collisions between strong winds of massive stars [1, 2, 3, 4], and is localized within the core of the cluster that is about 9'' (~ 0.35 pc at 8 kpc) in radius [5]. Diffuse non-thermal X-ray emission, revealed by its bright fluorescent Fe K α 6.4 keV line emission, has been detected from a broad region around the cluster [3, 6, 7, 8, 9].

The core of the Arches cluster has been relatively well studied in the standard 2 – 10 keV energy band with the *Chandra* and *XMM-Newton* observatories. The origin of the non-thermal extended emission, whether it is produced by the photoionization of the cloud by X-ray photons or through excitation by CR particles, was considered in many relevant studies [7, 8, 9]. [10] analysed the long-term behavior of the Arches cloud over 13 years and reported a 30% decrease in Fe K α line and continuum flux of the cloud emission in 2012-2013, providing the evidence that the majority of the variable non-thermal emission is due to X-ray reflection. Despite LECD-only emission is almost excluded based on variability, one could expect that steady background level is a result of CR heating, while most of the varying emission is due to reflection. For this reason we continue to measure spectral shape of the Arches cloud non-thermal emission, which contains imprints of the emission mechanism.

To separate thermal emission of the Arches cluster and non-thermal emission of the surrounding molecular cloud with *NuSTAR* [11], we utilize 2D image analysis as demonstrated in [12]. Similar procedure was also applied by [13], who analysed *NuSTAR* data of local Seyfert 2 active galactic nucleus (AGN) NGC 5643 and successfully decoupled partially confused spectra of AGN core and ultra-luminous source located in the same galaxy. In this paper we present 2D image spectral extraction procedure in more details.

2. The standard approach

The canonical method of spectrum extraction from X-ray data implies selecting circular region around the source and the region with representative source-free background. Then the standard tools of a given X-ray mission extract events from the regions; calculate the exposure; apply corrections for the Point Spread Function (PSF), vignetting, dead-time, etc.; generate appropriate Response Matrix Files (RMFs) and Ancillary Response Files (ARFs); and finally assemble source and background Pulse Height Amplitude (PHA) files with updated header keywords for spectral modeling in one of the popular packages, e.g. XSPEC [14] or SHERPA [15]. The standard approach fails in complicated cases with non-uniform background or spatial confusion of the sources in the X-ray images. The spatial modelling both the emission of the sources and background provides natural solution to this problem, however requires more sophisticated algorithms.

3. 2D image fitting procedure

We first combined the *NuSTAR* data into sky mosaics in 15 energy bands logarithmically cov-

ering the *NuSTAR* working energy range 3 – 79 keV. Each data set contains counts and exposure map. In the following analysis we assume flat background, so we do not need non-uniform background map, normally produced as a separate map in the same pixel resolution. Additional map contains PSF extracted from the *NuSTAR* Calibration Data Base (CALDB), placed in the center of the map. We assume the same PSF shape over the considered energy range 3 – 79 keV.

We then constructed spatial model of the Arches cluster complex, which includes two 2D Gaussians. The first represents the cluster’s core emission, with the position fixed at the centroid coordinates measured in [9] and width fixed at 4'' FWHM (PSF smearing effect). The second Gaussian was aligned with the corresponding “halo” Gaussian component used in [9] to describe the extended cloud emission, setting the FWHM model parameter at 72''.4. We fixed sky positions of the Gaussians as described in [12]. Thus, the only amplitudes of the 2D Gaussians were free parameters. As mentioned above, we assume flat background over the detector image. The normalization parameter was estimated in the annulus $70'' < R < 130''$ around the cluster.

We use SHERPA modeling and fitting package, a part of CIAO software [16], to construct 2D models and fit them to data. SHERPA enables one to construct a complex models from simple definitions, e.g. our current model setup can be expressed as $psf(gauss2d.G1 + gauss2d.G2) * emap + const2d.bkg * emap$, where $psf(gauss2d.G1 + gauss2d.G2) * emap$ means convolution of two Gaussians $G1$ and $G2$ with the PSF multiplied by the exposure map $emap$, the constant background term bkg is added as $const2d.bkg * emap$. Note that the background is not convolved with the PSF.

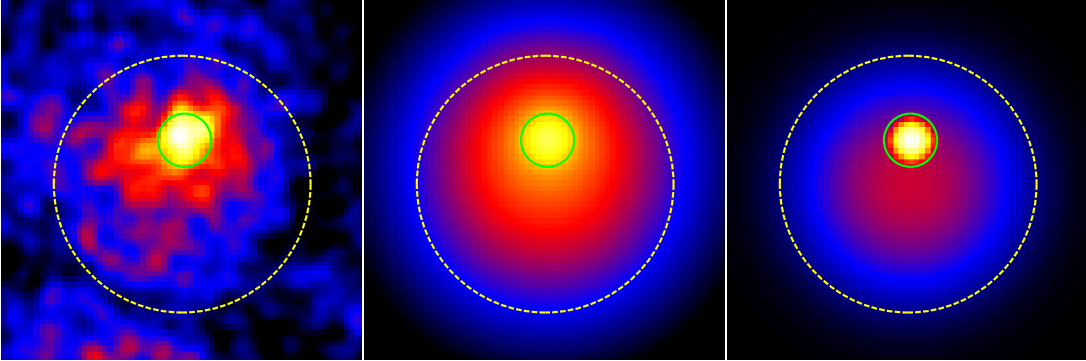


Figure 1: An example of 2D image fitting procedure of point-like Arches cluster’s core thermal emission (2D Gaussian model $G1$, 15' radius green circle) and the extended non-thermal emission of the surrounding molecular cloud (2D Gaussian model $G2$, yellow dashed 72''.4 FWHM radius circle). *Left:* *NuSTAR* image of the Arches cluster complex in 5.8 – 7.2 keV band, compatible with fluorescent iron line emission of the cloud ($G2$) at 6.4 keV and emission line of ionized iron at energy 6.7 keV of the cluster ($G1$). *Middle:* Best-fit spatial model of the Arches cluster complex in 5.8 – 7.2 keV band with two Gaussians $G1$ and $G2$ convolved with the *NuSTAR* PSF. *Right:* The same as middle plot, but not convolved with the PSF.

By running the fitting procedure in each of the 15 energy bands, we estimated the best-fitting parameters of the spatial models $G1$ and $G2$. We then calculated the flux, i.e. amount of collected photons with each model divided by the exposure time. The corresponding errors were estimated from multi-variate normal distribution, based on sampling the set of thawed parameters and calculating the model flux (*normal_sample* function in SHERPA). The estimated model fluxes and

uncertainties were combined into PHA spectra files of each spatial model $G1$ and $G2$ shown in Fig. 2. The corresponding Redistribution Matrix File (RMF), which maps from energy space into PHA space, was simply adopted from the standard spectral analysis of the ‘calibration’ source PMN J0641-0320 (see below) with *nuproducts* and rebinned with *rbrnmf* tool of HEASOFT 6.19 package.

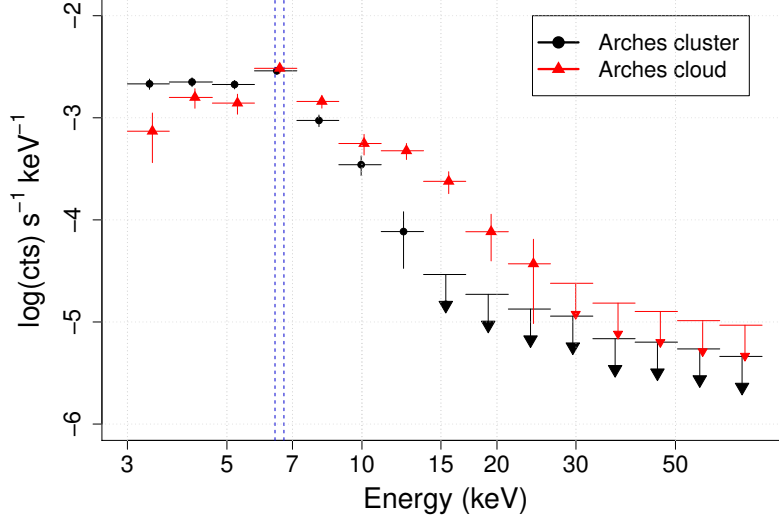


Figure 2: Spatially resolved *NuSTAR* spectra of the Arches cluster core (black) and cloud (red) X-ray emission. The position of Fe $K\alpha$ 6.4 and 6.7 keV are marked by vertical dashed lines, as in the *NuSTAR* standard spectra these two lines cannot be separated by our technique. The upper limits are 1σ errors.

As seen from Fig. 2, spatially confused emission of the Arches cluster complex was effectively decoupled with 2D image fitting procedure into the soft thermal emission of the cluster and hard non-thermal emission of the molecular cloud. Since the applied method uses the full collective power of the PSF, we could detect hard X-ray emission up to 20 – 30 keV. X-ray emission of the cluster contains an excess in the 5.8 – 7.2 keV range, compatible with ~ 6.7 keV line and rapidly drops above ~ 10 keV as expected for thermal emission with $kT \approx 2$ keV. Non-thermal emission of the extended cloud component apparently includes excess around 6.4 keV and dominates above 10 keV.

To use spatially decoupled $G1$ and $G2$ spectra in XSPEC spectral modeling package we calibrated effective area (ARF) utilizing the *NuSTAR* data of a bright source with known spectrum. To this end we used 20 ks observation (ObsID: 80001003002) of MeV Blazar PMN J0641-0320 with very hard power-law spectrum of $\Gamma \approx 1$ detectable up to ~ 80 keV [17]. We have done standard spectral extraction (Sect. 2) of PMN J0641-0320 within $70''$ radius circle, and estimated source flux $\text{phot s}^{-1} \text{cm}^{-2}$ in each of the 15 energy bands. We then repeated 2D image spectral extraction procedure (Sect. 3) for PMN J0641-0320 as a point-like source (one 2D Gaussian with $4''$ FWHM size) and estimated model flux phot s^{-1} in each of the 15 energy bands. Comparing the model fluxes obtained by two methods, we extracted the effective area in cm^{-2} for each band and combined them into ARF file. We should note that here we assume that the ARF calibrated for a point-like source is suitable for the extended emission of the Arches cloud. Given the limited

statistics of the *NuSTAR* Arches cluster observations, the deviations are within the uncertainties.

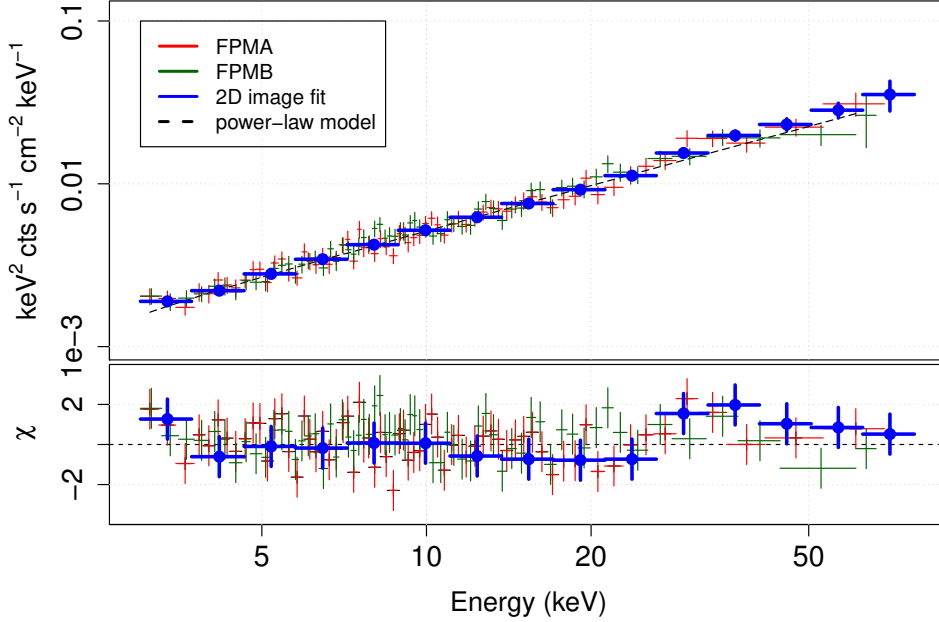


Figure 3: *NuSTAR* spectrum of MEV blazar PMN J0641-0320 extracted from $R = 70'$ circular region with standard procedures (red and green), and spectrum obtained through 2D image analysis (blue) described in this paper.

Fig. 3 shows X-ray spectra of MeV Blazar PMN J0641-0320 obtained with standard method (Sect. 2) for two *NuSTAR* modules FPMA and FPMB, and combined FPMA+FPMB spectrum extracted with 2D image algorithm (Sect. 3). It is seen that spectra are consistent with each other, demonstrating reliability of the 2D image fitting approach.

4. Results

The final spatially decoupled spectra of the Arches stellar cluster and extended molecular cloud emission is shown in Fig. 4. We fitted the stellar cluster emission spectrum with one APEC model subjects to a line-of-sight photoelectric absorption fixed at $N_H = 9.5 \times 10^{22} \text{ cm}^{-2}$. This simple model provides an acceptable fit to the data with $\chi_r^2/\text{d.o.f.} = 0.66/13$. We estimated two parameters from the fit: the temperature of the plasma $kT = 2.44 \pm 0.40 \text{ keV}$ and the unabsorbed 3 – 8 keV flux $(8.70 \pm 0.70) \times 10^{-13} \text{ erg s}^{-1} \text{ cm}^{-2}$.

The emission of the Arches cluster extended emission was approximated with power-law model and a Gaussian line with position and width fixed at 6.4 keV and 0.1 keV, respectively. The model gives acceptable fit statistics $\chi_r^2/\text{d.o.f.} = 1.02/12$ and allows for a constraint on the power-law slope $\Gamma = 2.06 \pm 0.26$ and the unabsorbed 3 – 20 keV flux $F_{3-20} = (9.33 \pm 1.34) \times 10^{-13} \text{ erg s}^{-1} \text{ cm}^{-2}$. The total flux of the 6.4 keV Gaussian line was estimated to be $(1.38 \pm 0.50) \times 10^{-5} \text{ photons cm}^{-2} \text{ s}^{-1}$.

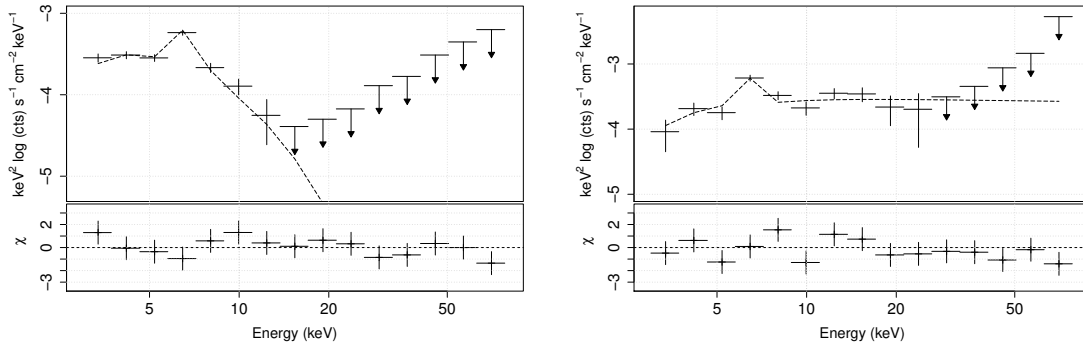


Figure 4: Spatially decoupled *NuSTAR* spectrum of the Arches cluster complex obtained with 2D image fitting procedure. *Left:* thermal spectrum of the Arches stellar cluster (*APEC*, $kT \sim 2$ keV). *Right:* non-thermal X-ray spectrum of the Arches molecular cloud extended emission, approximated with power-law model and iron 6.4 keV line represented with Gaussian.

5. Summary

In this work we presented details of the 2D image analysis approach used to decouple spatially confused emission components in the Arches cluster complex [12], namely, thermal emission of the stellar cluster and surrounding extended non-thermal emission of the molecular cloud. We demonstrated the capability of the method to decouple spatial emission components and validated its reliability in comparison with standard approach.

Acknowledgments

RK acknowledges support from the Russian Basic Research Foundation (grant 16-02-00294), the Academy of Finland (grant 300005) and hospitality of the Tuorla Observatory.

References

- [1] Chlebowski, T., & Garmany, C. D. 1991, *ApJ*, 368, 241
- [2] Yusef-Zadeh, F., et al. 2002, *ApJ*, 570, 665
- [3] Wang, Q. D., Dong, H., & Lang, C. 2006, *MNRAS*, 371, 38
- [4] Capelli, R., et al. 2011a, *A&A*, 525, L2
- [5] Figer, D. F., et al. 1999, *ApJ*, 525, 750
- [6] Tsujimoto, M., Hyodo, Y., & Koyama, K. 2007, *PASJ*, 59, 229
- [7] Capelli, R., et al. 2011b, *A&A*, 530, A38
- [8] Tatischeff, V., Decourchelle, A., & Maurin, G. 2012, *A&A*, 546, A88
- [9] Krivonos R. A., et al., 2014, *ApJ*, 781, 107
- [10] Clavel M., et al. 2014, *MNRAS*, 443, L129
- [11] Harrison, F. A., et al. 2013, *ApJ*, 770, 103
- [12] Krivonos, R., et al. 2017, arXiv:1612.03320
- [13] Krivonos, R., & Sazonov, S. 2016, *MNRAS*, 463, 756
- [14] Arnaud, K. A. 1996, *Astronomical Data Analysis Software and Systems V*, 101, 17
- [15] Freeman, P., Doe, S., & Siemiginowska, A. 2001, *Proc. SPIE*, 4477, 76
- [16] Fruscione, A., et al. 2006, *Proc. SPIE*, 6270,
- [17] Ajello, M., et al. 2016, *ApJ*, 826, 76